ON THE ACOUSTIC HEATING OF THE POLAR NIGHT MESOSPHERE

KAICHI MAEDA

A Reprint from

APRIL 1, 1964

Journal of Geophysical Research

VOLUME 69 NUMBER 7

PUBLISHED BY
THE AMERICAN GEOPHYSICAL UNION

JOURNAL OF GEOPHYSICAL RESEARCH VOL. 69, NO. 7 APRIL 1, 1964

On the Acoustic Heating of the Polar Night Mesosphere

KAICHI MAEDA

21205

Goddard Space Flight Center, Greenbelt, Maryland

Abstract. As a part of the dynamical heating emphasized by Hines, the contribution of aerodynamically produced atmospheric acoustic waves to the warming of the polar night mesosphere is re-examined with the polar night jet stream in the stratosphere as the source, and with the thermal structure of the polar upper atmosphere playing a part in propagation and absorption. It is shown that owing to the relatively small transmissivity of the thermosphere for long-period sound waves, most acoustic heating does not take place above the 200-km level, but rather below 100 km, or around the mesopause, and that although acoustic output power from the polar jet stream is more than 10^5 times larger in winter than in summer, acoustic heating is not sufficient to compensate for the cooling rate around the mesopause in winter, unless the wind velocity of the polar night jet stream continually exceeds 200 m/sec.

Author author

INTRODUCTION

An effective heating mechanism for the polar mesosphere, which is warmer in winter than in summer, is Kellogg's chemical heating through the recombination of atomic oxygen [*Kellogg*, 1961; *Young and Epstein*, 1962; *Maeda*, 1963]. Although the velocity of subsidence required for this process is significantly less than that required for adiabatic heating alone, it must still be of the order of 0.1 cm/sec near the 60- to 90-km level.

On the other hand, theoretical calculations by *Haurwitz* [1961] indicate an upward rather than a downward flow in this region. And although R. Sawada (private communication, 1961) has questioned Haurwitz's omission of certain inertia terms in his basic equations, a recent analysis by *Kochanski* [1963] of rocket data relating to mesospheric circulation shows good agreement with Haurwitz's results.

Rocket soundings by *Nordberg and Smith* [1963] have occasionally measured very warm wintertime mesosphere temperatures even in the middle latitudes where subsidence is unlikely, but where very strong westerlies in the region 40–80 km appear to be associated.

Hines [1962] has suggested that the increase of temperature in the polar night mesosphere could be explained by dynamical heating. *Gossard* [1962] and *Blamont and De Jager* [1961] have found evidence of upward propagation of tropospheric disturbances into the ionosphere.

The possibility of acoustic heating of the ionosphere was discussed by *Daniels* [1952], who considered noise produced by the sea surface as an energy source. However, *Eckart* [1953] showed that pressure waves from this source are completely ineffective in transferring energy up to such high altitudes. This has recently been confirmed by *Cook and Young* [1963]. The amount of acoustic heating of the ionosphere was also estimated by *Golitsyn* [1961*b*], using tropospheric sources. He arrived at an upward energy flux of the order of 10^{-3} erg cm^{-2} sec, which is insufficient to cause the observed heating. Moreover, he did not consider the reflection of acoustic energy due to the vertical temperature distribution in the atmosphere.

In this paper, the contribution of aerodynamically produced atmospheric acoustic waves to the warming of the polar night mesosphere is re-examined, with the polar night jet stream in the stratosphere as the source, and with the thermal structure of polar upper atmosphere playing a part in propagation and absorption.

It should be noted that the largest part of the kinetic energy of the atmosphere is in the troposphere, where the air density is greatest, and is of the order of 10^3 ergs cm^{-3}. If this tropospheric kinetic energy is not trapped effectively within the troposphere, the earth's atmosphere at ionospheric heights should reach very high temperatures of the order of 10^5 °K. However, *Charney and Drazin* [1961] have shown that

the escape of large amounts of planetary wave energy from the tropospheric layer into the upper atmosphere is prevented throughout most of the year by the large westerly zonal wind systems above the tropopause, except for short periods in the spring and autumn.

Kinetic Energy Density of the Polar Statosphere

Owing to the polar night vortex and jet stream, the kinetic energy of the polar stratosphere increases remarkably during polar nights. As may be in the case of the solar corona, some part of this kinetic energy may be transferred upward by means of internal pressure waves. According to *Boville et al.* [1961], the kinetic energy density of zonal wind systems between 60 and 80°N at 25 and 500 mb increases significantly during the wintertime (from December until March). The kinetic energy density corresponding to the winter peak of the basic zonal flow is of the order of 150 and 600 ergs cm^{-3} at the 25- and 500-mb levels, respectively. For example, the increase of kinetic energy at Ft. Churchill during the period of July 1957 to July 1958 (Figure 1) [*U. S. Weather Bureau,* 1961] in the upper stratosphere in wintertime is caused mainly by the development of the polar night jet stream [*Krishnamurti,* 1959].

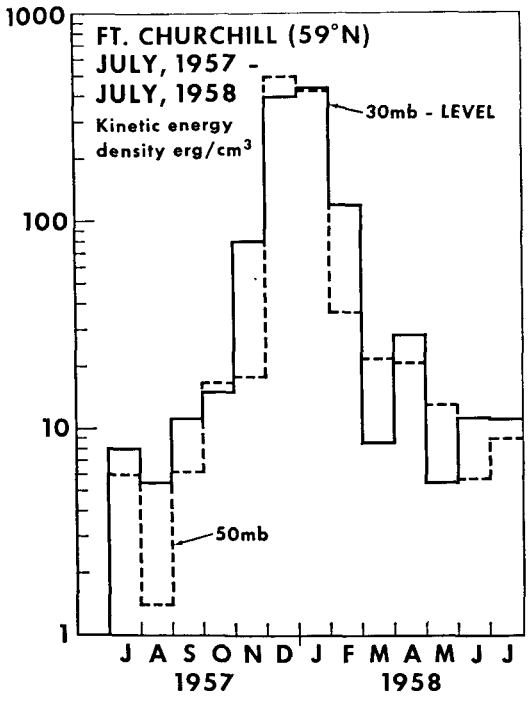

Fig. 1. Monthly average of kinetic energy density at 30 mb (solid lines) and at 50 mb (dashed lines) during the period from July 1957 to July 1958 above Ft. Churchill (59°N geographic latitude) in ergs cm^{-3}.

The dissipation of the energy of jet streams, as well as any strong wind system in the atmosphere, is mainly due to friction in the boundary layers, which cause turbulent motion to decay into small eddies in the surrounding mediums. These eddies decay further into thermal motion and cause local heating. However, some part of the kinetic energy in turbulent motion in jet flow can propagate into the upper atmosphere in the form of pressure waves. Owing to the exponential decrease of air density with height, the amplitudes of those propagating pressure waves grow rapidly in high altitudes and approach shock-wave magnitudes; i.e., dissipation becomes nonlinear.

The propagation and absorption properties and energies of these internal atmospheric waves are discussed mathematically in the next section.

Equations of Internal Atmospheric Waves

The notations and constants.

a^2, thermal conductivity of air, i.e., $a^2 = \kappa/C_p\rho$ in cm^2/sec.

c, sound velocity in the air, km/sec.

D/Dt, the Eulerian derivative, i.e., $\partial/\partial t + \nabla\cdot\mathbf{V}$.

$\mathbf{f}$, resultant of all external forces.

g, acceleration of gravity, $9.8\cdot10^{-3}$ km sec.$^{-2}$

H, scale height of isothermal atmosphere, i.e., $H = RT_0/g$.

J_0, Joule's mechanical equivalent of heat, $4.185\cdot10^7$ ergs/cal.

k, horizontal wave number, corresponding to λ, i.e., $\kappa = 2\pi/\lambda$, in km^{-1}.

p, ρ, T, small departure from static value of pressure, density, and temperature, function of x and z.

p_0, ρ_0, T_0, static pressure, density, and absolute temperature which are the functions of z only in dynes/cm^2, g/cm^3, and °K, respectively.

$\bar{p}$, $\bar{\rho}$, $\bar{T}$, total pressure, density, and absolute temperature, i.e., $\bar{p} = p_0 + p$, $\bar{\rho} = \rho_0 + \rho$, and $\bar{T} = T_0 + T$.

R, gas constant of air, $2.87\cdot10^{-4}$ km^2 sec^{-2} °K^{-1}.

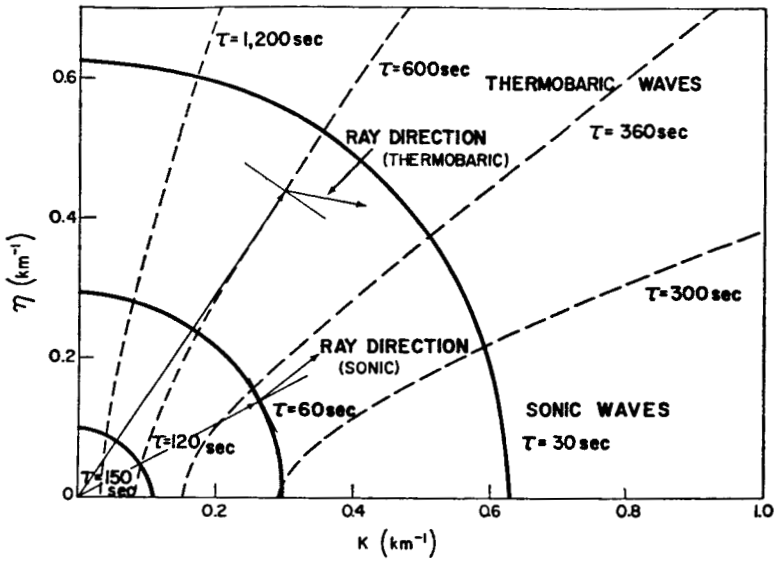

Fig. 2. Propagation surfaces (heavy lines) of internal atmospheric wave in the isothermal atmosphere with scale height 8 km ($T_0 = 0°C$), given by (12); heavy lines and dashed lines correspond to sonic waves (acoustic waves) and thermobaric waves (internal gravity waves), respectively.

$\mathbf{V}(u, w)$, velocity vector, where u is horizontal (southward) and w is vertical (upward) component of air motion in m/sec.

z, period of pressure wave.

γ, ratio of specific heats of air C_p/C_v, where C_p and C_v are the specific heat of air at constant pressure and that at constant volume, respectively.

κ, heat conductivity of air in cal/cm sec °K.

λ, horizontal wavelength of pressure wave, in km.

μ, viscosity of air, in dynes sec/cm².

ν, kinematic viscosity of air, i.e., $\nu = \mu/\rho_0$ in cm²/sec.

τ, period of pressure wave in sec.

$\chi(x, z)$, the divergence of velocity in sec⁻¹, i.e., $\chi = \partial u/\partial x + \partial w/\partial z$ where x and z are horizontal (southward) and vertical (upward) coordinate, respectively.

ω, angular frequency of pressure wave corresponding to τ, $2\pi/\tau$.

The fundamental equation. The equation of internal atmospheric waves is derived from the following three fundamental equations: namely, the equation of motion

$$\frac{D\mathbf{V}}{Dt} + \frac{1}{\bar{\rho}} \nabla \bar{p} + \mathbf{g} = \mathbf{f} \qquad (1)$$

the equation of continuity

$$\frac{D}{Dt}\left(\frac{1}{\bar{\rho}}\right) = \frac{1}{\bar{\rho}} \nabla \cdot \mathbf{V} \qquad (2)$$

and the equation of thermodynamics

$$D\bar{p}/Dt = c^2(D\bar{\rho}/Dt) \qquad (3)$$

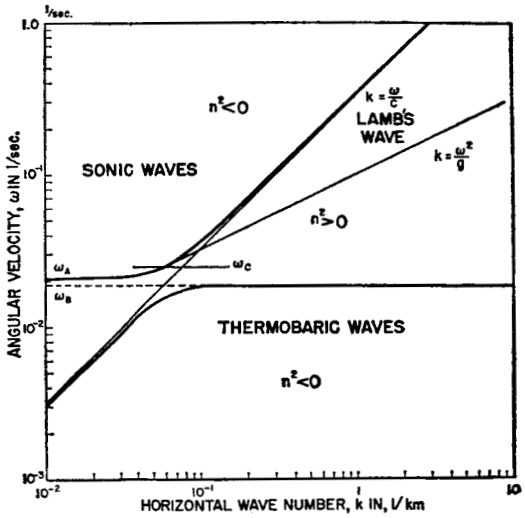

Fig. 3. Diagnostic diagram of internal atmospheric waves in the isothermal atmosphere with scale height 8 km ($T_0 = 0°C$); ordinate and abscissa are angular frequency ω in sec⁻¹ and horizontal wave number k in km⁻¹, respectively.

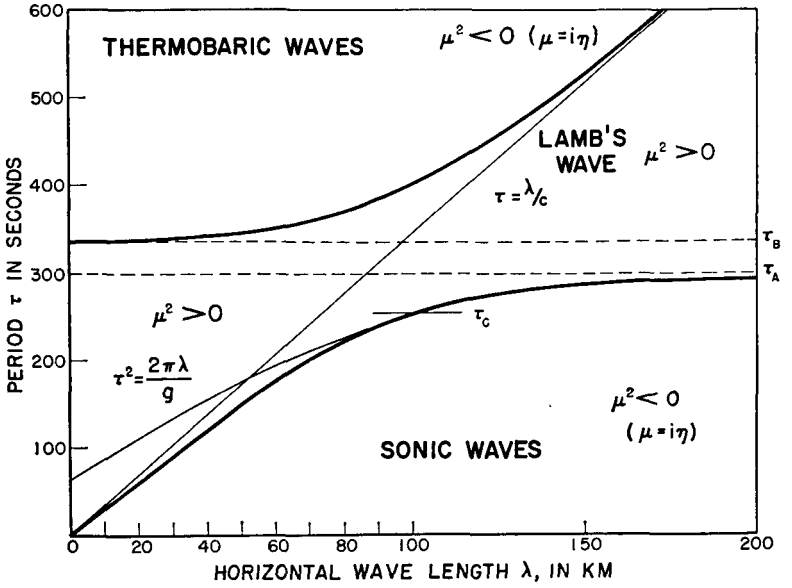

Fig. 4. Diagnostic diagram of internal atmospheric waves in the isothermal atmosphere with scale height 8 km ($T_0 = 0°C$), where ordinate abscissa are period τ in seconds and horizontal wavelength λ in kilometers, respectively. τ_A and τ_B correspond to the ω_A and ω_B of Figure 3, respectively.

Since the source of disturbance is extended along a certain latitude, the problem can be treated in two dimensions and the coordinates specified within a meridional plane. Let x be horizontal (southward) and z vertical (upward). In the first approximation, the Coriolis force and external forces, except gravity, are neglected. The equation of motion 1 then becomes

$$\rho_0(\partial u/\partial t) = -\partial p/\partial x$$

and

$$\rho_0(\partial w/\partial t) = -\partial p/\partial z - g\rho$$

The equation of continuity 2 for the first-order approximation is

$$\frac{\partial \rho}{\partial t} + w\frac{\partial \rho_0}{\partial z} = -\rho_0 \cdot \chi \qquad (4)$$

where $\chi = \chi(x, z, t)$ is the velocity divergence defined in the preceding section. By using (4), we can write the equation of thermodynamics 3 as

$$(\partial p/\partial t) + (c^2\chi - wg)\rho_0 = 0$$

The waves traveling in the flat atmosphere can be found by assuming that u, w, p, and ρ are proportional to $\exp(\omega t - kx)$. Then, by elimination of u, w, p, and ρ:

$$\frac{d^2\chi}{dz^2} + \frac{1}{c^2}\left(\frac{dc^2}{dz} - \gamma g\right)\frac{d\chi}{dz} + \left[\frac{\omega^2}{c^2} - k^2 + \frac{gk^2}{\omega^2 c^2} \cdot \left(\frac{dc^2}{dz} + (\gamma - 1)g\right)\right]\chi = 0$$

Since $c^2 = \gamma g H$, this is written further as

$$\frac{d^2\chi}{dz^2} + \frac{1}{H}(H' - 1)\frac{d\chi}{dz} + \left[\frac{\omega^2}{\gamma g H} - k^2 + \frac{k^2 g}{\omega^2 H} \cdot \left\{H' + \left(1 - \frac{1}{\gamma}\right)\right\}\right]\chi = 0 \qquad (5)$$

where $H' = dH/dz$.

The diagnostic diagram. The wave equation 5 can be written

$$\frac{d^2\chi}{dz^2} - 2N\frac{d\chi}{dz} + M^2\chi = 0 \qquad (6)$$

where

$$N = (1/2H)(1 - H') \qquad (7)$$

$$M^2 = \frac{\omega^2}{c^2} - k^2 + \frac{k^2 g}{\omega^2 H}\left(H' + 1 - \frac{1}{\gamma}\right) \qquad (8)$$

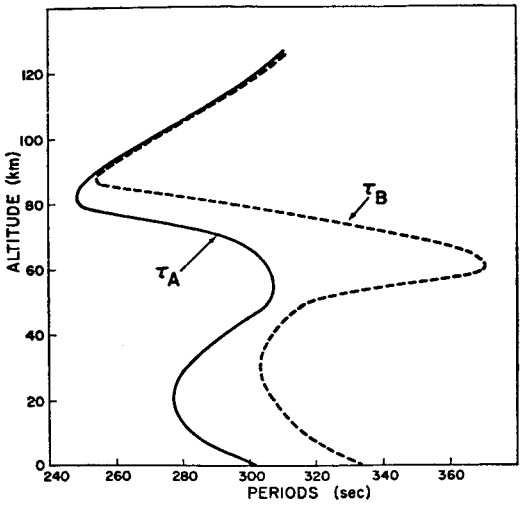

Fig. 5. Atmospheric resonant sound period τ_A and Brunt-Väisälä period τ_B as a function of altitude for the polar atmosphere in summer.

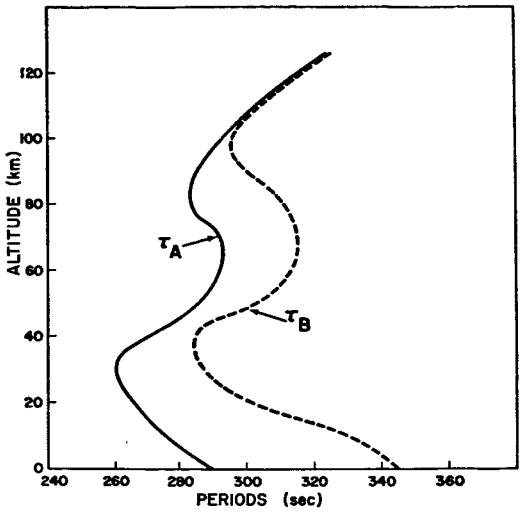

Fig. 6. Atmospheric resonant sound period τ_A and Brunt-Väisälä period τ_B as a function of altitude for the polar atmosphere in winter.

Solution of the differential equation 6 is given approximately by

$$\chi(x, z) = e^{Nz}(Ae^{-nz} + Be^{+nz}) \qquad (9)$$

where A and B are constant and can be determined by boundary conditions.

It should be noted that the solution 9 of (6) or (5) can be classified as cellular and noncellular,[1] depending on the relative magnitudes of N and M; i.e.,

1. The cellular solution:

$$n = i\eta \qquad \eta^2 = M^2 - N^2 \quad \text{for} \quad M^2 > N^2 \qquad (10)$$

2. The noncellular solution:

$$n^2 = N^2 - M^2 \quad \text{for} \quad N^2 < M^2 \qquad (11)$$

The cellular waves have propagation vectors in both the horizontal (k) and vertical (η) directions, while noncellular waves have no propagation vector in the vertical direction and simply propagate in the horizontal direction.

Since M is a function of the horizontal wave number k, (10) gives the relation between two wave numbers in the vertical (η) and in horizontal direction (k):

$$\frac{\eta^2 c^2}{\omega^2 - \omega_A^2} + \frac{k^2 c^2(\omega^2 - \omega_B^2)}{\omega^2(\omega^2 - \omega_A^2)} = 1 \qquad (12)$$

where

$$\omega_A^2 = \left(\frac{\gamma g}{2c}\right)^2 \cdot \left(1 - \frac{1}{\gamma g}\frac{dc^2}{dz}\right) \qquad (13)$$

or

$$\omega_A = \frac{c}{2H}(1 - H')^{1/2}$$

$$\omega_B^2 = \frac{g}{c^2}\left(\frac{dc^2}{dz} + (\gamma - 1)g\right) \qquad (14)$$

or

$$\omega_B = \sqrt{g}\sqrt{\frac{H'}{H} + \frac{1}{H}\left(1 - \frac{1}{\gamma}\right)}$$

ω_A and ω_B are called the atmospheric resonant sound angular frequency and Brunt-Väisälä angular frequency, respectively [*Tolstoy*, 1963]. These frequencies are both functions of the atmospheric temperature distribution in the vertical direction and are related to the stability of layers in the atmosphere.

We can see from (12) that the propagation surface is an ellipsoid if $\omega > \omega_A$, but it is a hyperboloid if $\omega < \omega_B$. In the former case the waves are called sonic or acoustic waves and in

[1] The nomenclature of cellular and noncellular is taken from *Martyn's* [1950] paper, and these terms correspond to internal and external waves discussed by *Charney and Drazin* [1961].

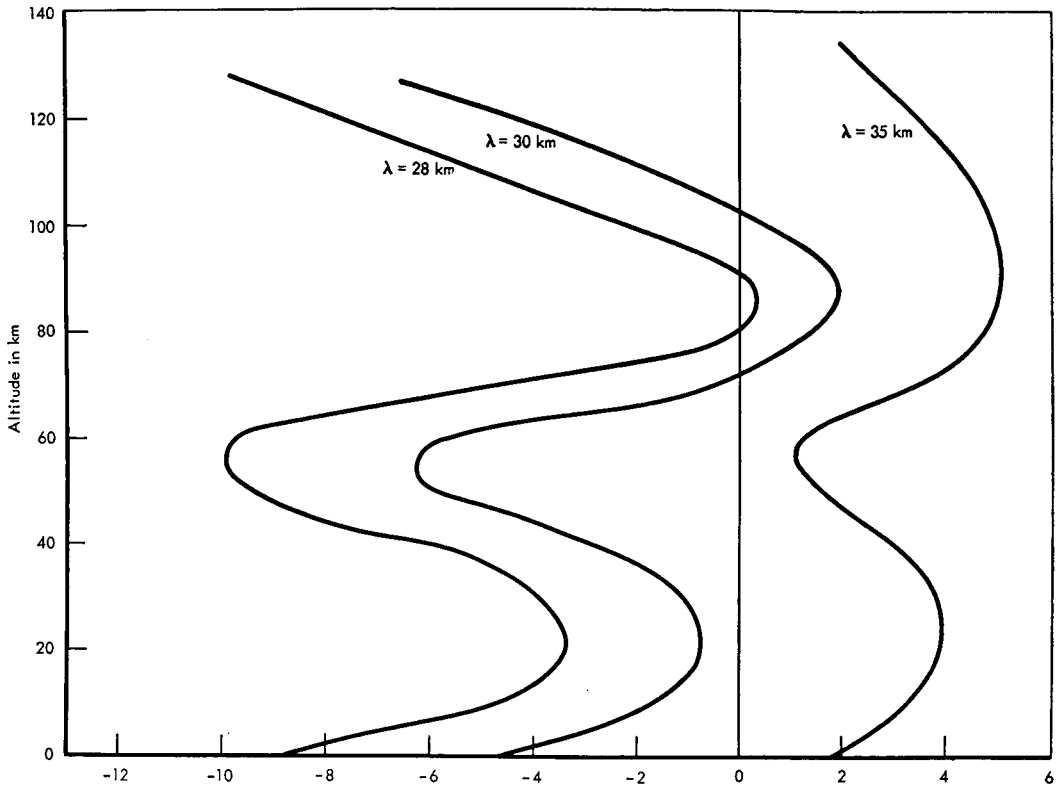

Fig. 7*a*. Square of the index of refraction K^2 for atmospheric acoustic waves with period τ in the summertime polar atmosphere as a function of height, where the parameter λ is the horizontal wavelength in kilometers and $\tau = 100$ sec.

the latter thermobaric [*Eckart*, 1960] or internal gravity waves [*Hines*, 1960] (Figure 2). In both cases, the rotation axis is vertical (z axis).

Since η^2 becomes negative for $\omega_B < \omega < \omega_A$, no cellular wave exists for this frequency range (see Figures 3 and 4). These figures are called diagnostic diagrams of atmospheric waves [*Eckart*, 1960], in which a domain indicated by $n^2 > 0$ corresponds to the noncellular mode and two-domain $n^2 < 0$ (i.e., $\eta^2 > 0$) stands for the cellular modes.

Approximate Transmissivity of the Polar Atmosphere

Since the noncellular (or external) waves, whose periods are between τ_A and τ_B, have no vertical propagation vector, these waves neither contribute to vertical energy transfer nor exist locally in free atmosphere. For cellular (or internal) waves, on the other hand, the thermobaric (or internal gravity) mode can propagate with a period larger than Brunt period τ_B, but sonic (or acoustic) modes exist only below a period τ_A.

As can be seen from (13) and (14), these two critical periods are a function of the atmospheric temperature and the vertical temperature gradient in the atmosphere (i.e., lapse rate of atmospheric temperature). Therefore, these values must differ not only with height, but also with season (Figures 5 and 6).

The atmospheric models for the two seasons are essentially the same as the ones reported by *Stroud et al.* [1960] [see also *Maeda*, 1962, Figure 13; *Young and Epstein*, 1962, Figure 1]. In a domain between two critical periods, i.e., τ_A (solid line) and τ_B (dashed line), only the noncellular mode can exist. Therefore no thermobaric waves with a period shorter than 370 sec can propagate across the 50-km level and no sonic waves with a period longer than 250 sec can propagate through the 80-km layer in

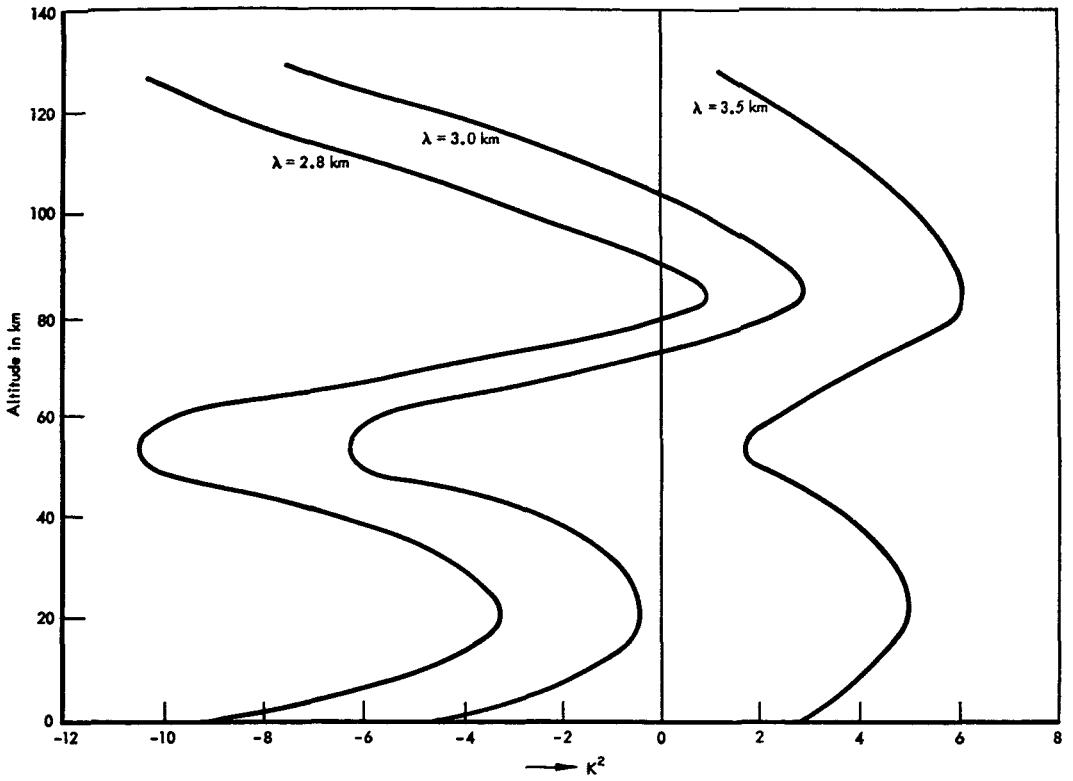

Fig. 7b. Square of the index of refraction K^2 for atmospheric acoustic waves with period τ in the summertime polar atmosphere as a function of height, where the parameter λ is the horizontal wavelength in kilometers and $\tau = 10$ sec.

summer. In winter both waves are able to propagate through these layers and the critical periods approach each other: 320 sec for thermobaric waves and 290 sec for sonic waves.

To see the transparency (or transmissivity) of the atmosphere for internal waves more quantitatively, the wave equation 6 should be transformed into a more simple form. By substituting for z

$$y = \int_{z0}^{z} dz/H$$

and

$$\chi(z) = e^{y/2}\phi(y)$$

the term $d\chi/dz$ in the wave equation can be eliminated. Then (6) is written as

$$d^2\phi(y)/dy^2 = -K^2\phi(y) \qquad (15)$$

where

$$K^2 = \eta^2 \cdot H^2$$

As can be seen from (7), (8), and (10), η^2 is a function of ω, k, H, and H'.

The one-dimensional wave equation 15 indicates that, if $K^2 > 0$, the solution $\omega(y)$ has a wave nature, and corresponding waves can propagate along the vertical direction, within the domain, where this condition is satisfied. On the other hand, from Figure 2 we can see that there is a shortest (critical) horizontal wavelength λ_c for a given period of the waves which corresponds to a largest horizontal wave number k_c, and that the wave propagating close to vertical direction has longer horizontal wavelength than the one propagating in an oblique direction with the same period of the wave. In Figures 7 and 8, therefore, the waves propagating close to vertical axis can propagate upward as far as $\tau < \tau_A$, while the waves propagating obliquely meet a barrier, where, even if the condition $\tau < \tau_A$ is satisfied, K^2 becomes negative. If there are more than two barriers, those obliquely propagating waves are trapped between these barriers, form-

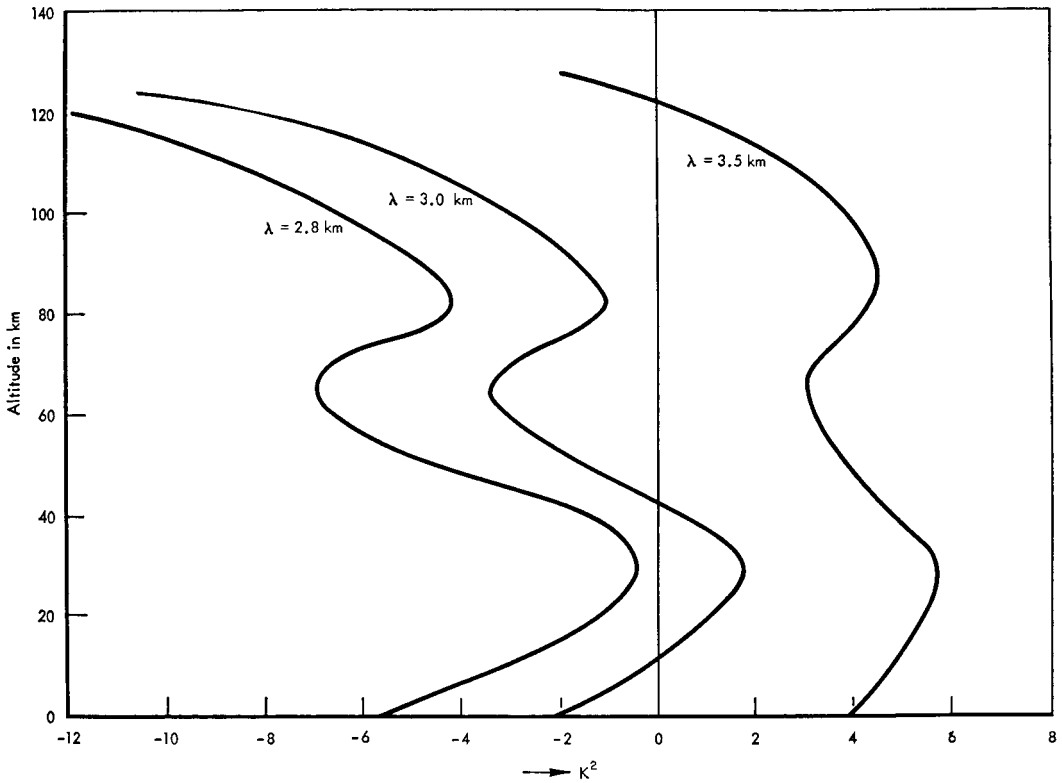

Fig. 8*a*. Curves similar to Figure 7*a* for wintertime polar atmosphere; $\tau = 100$ sec.

ing a duct in the horizontal direction. By comparing Figures 7 and 8, we find the barriers to be weaker in winter than in summer.

Using the diagram shown in Figure 2, for the conditions at each level the critical angle θ_c can be drawn as a function of altitude for a given period τ of the waves, provided that $\tau < \tau_A$. θ_c is defined such that the waves propagating obliquely with zenith angle larger than θ_c cannot enter into the above layer, simply because K^2 becomes negative beyond this angle. In other words, θ_c can be regarded as the aperture of allowed cone around the vertical axis at each level in the atmosphere. Therefore the relative transmissivity $f_t(\tau, z)$ of each layer for vertical propagation of atmospheric acoustic wave is given approximately by $(2\theta_c/\pi)^2$, provided that θ_c is expressed in radians. From Figure 9, it is seen that the atmosphere above the mesopause, which is nearly 80 km in the polar region, is always opaque for the atmospheric acoustic waves. It should be noted that the wind system in the higher layers is not affected very much by the relative transmissivity, because an oblique axis tilted windward can be regarded as the direction of maximum propagation.

Upward Energy Transfer by Pressure Waves

Acoustic waves generated aerodynamically in the atmosphere. Sound waves generated aerodynamically are different from sound waves produced by the vibration of solids. A strong jet flow in the free atmosphere produces sound waves due to turbulent motions in the boundary layers between the core of a jet and surrounding air. *Lighthill* [1951, 1954] investigated this problem and derived a theoretical expression for the power of sound waves as a function of jet stream velocity. His theory was further extended by *Proudman* [1952] to the generation of sonic waves by isotropic turbulence.

Although the acoustic heating of the solar corona is discussed by *Schatzman* [1961], similar calculations cannot be applied to the earth's atmosphere, because the situation in the earth's

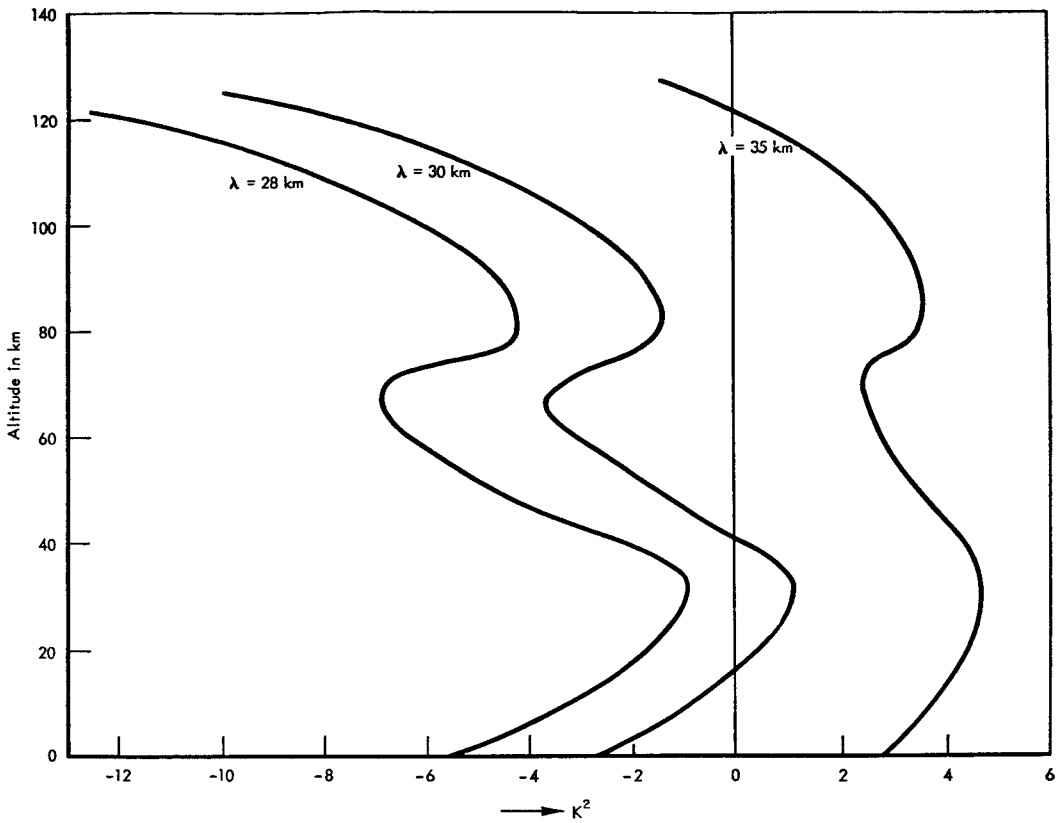

Fig. 8*b*. Curves similar to Figure 7*b* for wintertime polar atmosphere; $\tau = 10$ sec.

upper atmosphere is entirely different from that of solar atmosphere. As was discussed by *Kulsrud* [1954], the effect of magnetic fields on the generation of sound noise by isotropic turbulence is important as well as on the dissipation processed in the case of solar corona.

Since the aerodynamical production of acoustic waves has been developed in detail by Lighthill and Proudman, here only their results will be applied to the present problem in the earth's upper atmosphere. The acoustic power output per unit mass of air P, in ergs/g sec, is given by

$$P = \alpha \epsilon M^5 \quad \text{for} \quad M \ll 1 \qquad (16)$$

where α is a nondimensional constant, ϵ is the mean rate of energy dissipation per unit mass, and the Mach number $M = u/c$ (u and c are the mean velocity of jet flow and sound velocity, respectively).

According to *Batchelor* [1956, p. 103], ϵ is given by

$$\epsilon(\cong du^2/dt) = A\bar{u}^3/l$$

where A is a nondimensional constant of the order of unity, l is a characteristic length, which can be taken as the reciprocal of the wave number at which the maximum of the energy spectrum occurs, and $\bar{u}$ is the root mean square velocity of turbulence.

If the double correlation function given by *Heisenberg* [1948] is correct, the constant α in (16) is numerically 38. Then (16) can be written

$$P \cong (70\bar{u}^3/l)(M)^5$$

In the upper atmosphere, where the Reynolds number is very large, the spectrum of turbulence consists generally of three ranges:

1. The energy-producing range, which contains large eddies.
2. The inertial subrange in which energy is neither created nor destroyed.
3. The energy-dissipating range, which contains small eddies.

As *Proudman* [1952] pointed out, the turbu-

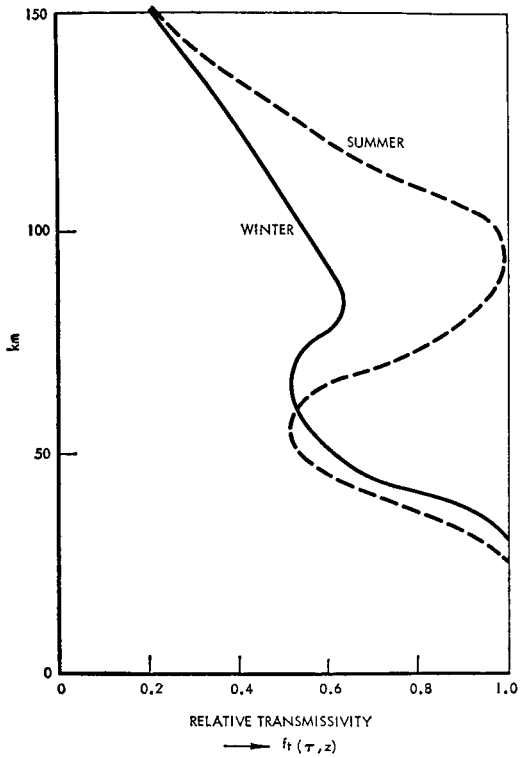

Fig. 9. Relative transmissivity of polar atmosphere, $f_t(\tau, z)$, for atmospheric acoustic wave with a period $\tau = 100$ sec; solid line and dashed line correspond to wintertime and summertime, respectively.

lence which makes an appreciable contribution to the generation of sonic waves at large Reynolds number belongs to the eddies that do not dissipate energy. In other words, the main source of aerodynamically produced sonic waves is turbulent motion around jet flow, which belongs to (1) the energy maintaining range, and to (2) the inertial subrange. Therefore, according to *Batchelor* [1956, chapter 7], the following assumption can be made:

$$10^3 \lesssim l \lesssim 10^4 \quad \text{and} \quad 1/10 \lesssim \bar{u}/u \lesssim 1/3$$

The distribution of turbulence along the jet stream can be assumed uniform; then the acoustic output per unit area along the jet $I(u)$, in ergs/cm² sec, will be

$$7.10^{-6}u^3M^5\rho_0 \lesssim I(u) \lesssim 3.10^{-3}u^3M^5\rho_0 \quad (17)$$

where ρ_0 is mean density of air around the source.

From Figure 10 the production of sonic waves is seen to decrease drastically below a wind velocity u of the order of 50 m/sec. Since the derivation of (17) is based on the assumption that the Mach number is small [*Lighthill*, 1954], calculations with the output power beyond $u = 150$ m/sec might be incorrect.

Attenuation of atmospheric waves. As has been shown, the propagation of atmospheric sonic waves is nearly isotropic if the wavelength or period is very short, while thermobaric waves propagate almost horizontally. However, if the wavelength (or period) increases, transmissivity in the vertical direction decreases. On the other hand, any atmospheric waves are attenuated in air by the following methods: (1) friction due to viscosity of air, (2) thermal conduction of air, (3) radiation through the atmosphere, (4) dispersion due to the inhomogeneity of air in the atmosphere. Neglecting effects of (3) radiation

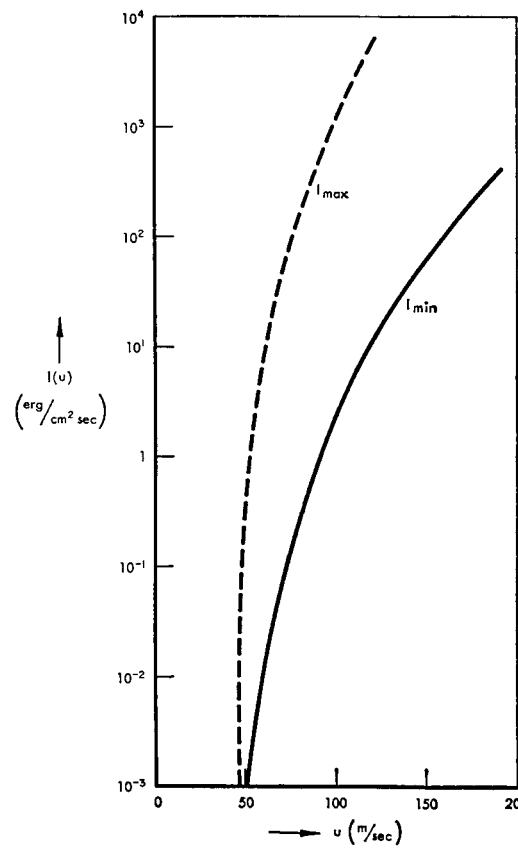

Fig. 10. Acoustic output power of the polar stratosphere $I(u)$, in ergs/cm² sec, with an assumed source height of 25 km, plotted against the mean wind velocity of the jet stream u in m/sec.

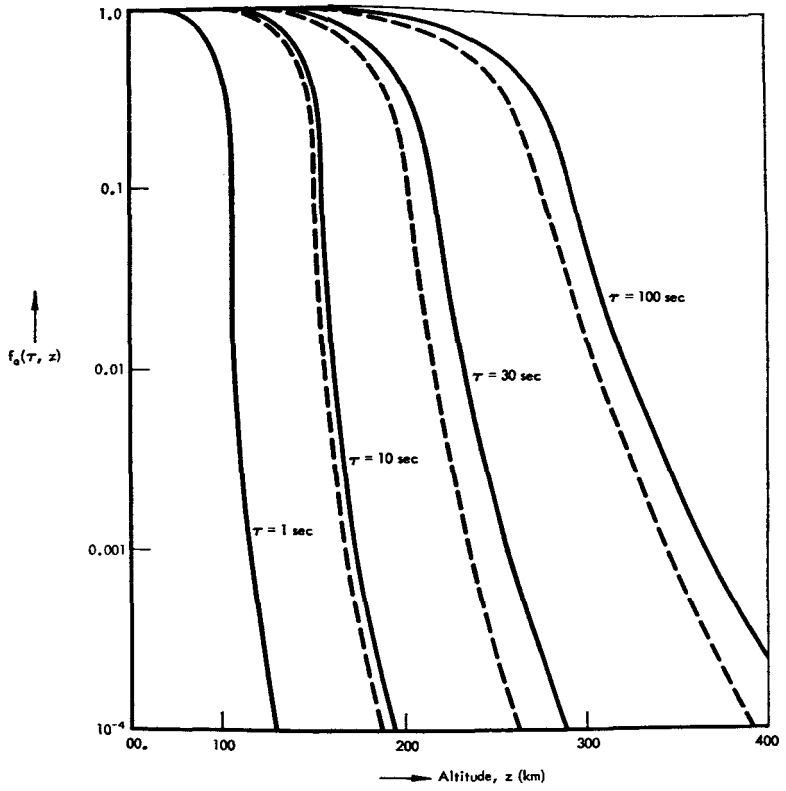

Fig. 11. Attenuation factor $f_a(\tau, z)$ of atmospheric acoustic wave versus altitude z for $\tau = 1$, 10, 30, and 100 sec. Solid lines are calculated by the classical formula 18 and dashed lines are given by *Golitsyn* [1961*a*], taking Joule loss in the ionosphere into account.

and (4) dispersion, which are generally small for acoustic waves as compared with the effects of (1) friction and (2) thermal conduction, we get the so-called classical Stokes-Kirchhoff formula for the attenuation coefficient $\alpha(\tau)$ [*Schrödinger*, 1917; *Rayleigh*, 1945], which is given by

$$\alpha(\tau) \cong \frac{4\pi^2}{\tau^2 c^3}\left\{\frac{\gamma - 1}{\gamma}\, a^2 + \frac{4}{3}\nu\right\} \qquad (18)$$

where $a^2 = K/C_v\, \rho$ and $\nu = \mu/\rho$. The heat conductivity of air κ is of the order of 6×10^{-6} cal/cm sec °K at NTP, and the specific heat C_v is nearly 0.27 cal/g °K below the mesopause and increases with height to 0.3 cal/g °K above approximately 350 km [*Ishikawa*, 1959]. The viscosity of air μ is of the order of 1.7×10^{-4} poise at NTP. By using these numerical values, we can write the attenuation coefficient (equation 18), in cm^{-1},

$$\alpha(\tau) \cong (2.4 \times 10^{-16})/\rho\tau^2$$

As *Golitsyn* [1961*a*] showed, long-period pressure waves undergo an additional dissipation owing to Joule loss of the current induced by fluctuations of the conducting medium of the ionosphere in the earth's magnetic field.

In Figure 11, the attenuation factor

$$f_a(\tau, z) = \exp\left[-\int_0^z \alpha(\tau, z')\, dz'\right] \qquad (19)$$

is shown for four different wave periods.

An estimate of the rate of energy dissipation per unit time per unit thickness per unit cross section in the upper atmosphere is made by the following approximation:

$$\frac{dE_t}{dz} \cong \int_{\omega_A(z)}^{\infty} i(\omega) f_t(\omega, z)\, \frac{d}{dz} f_a(\omega, z)\, d\omega \qquad (20)$$

where dE_t/dz is in ergs/cm³ sec, and $f_a(\omega, z)$, the attenuation factor, is given by (19) and shown in Figure 11. $f_t(\omega, z)$ is relative transmissivity of atmosphere as shown in Figure 9. The

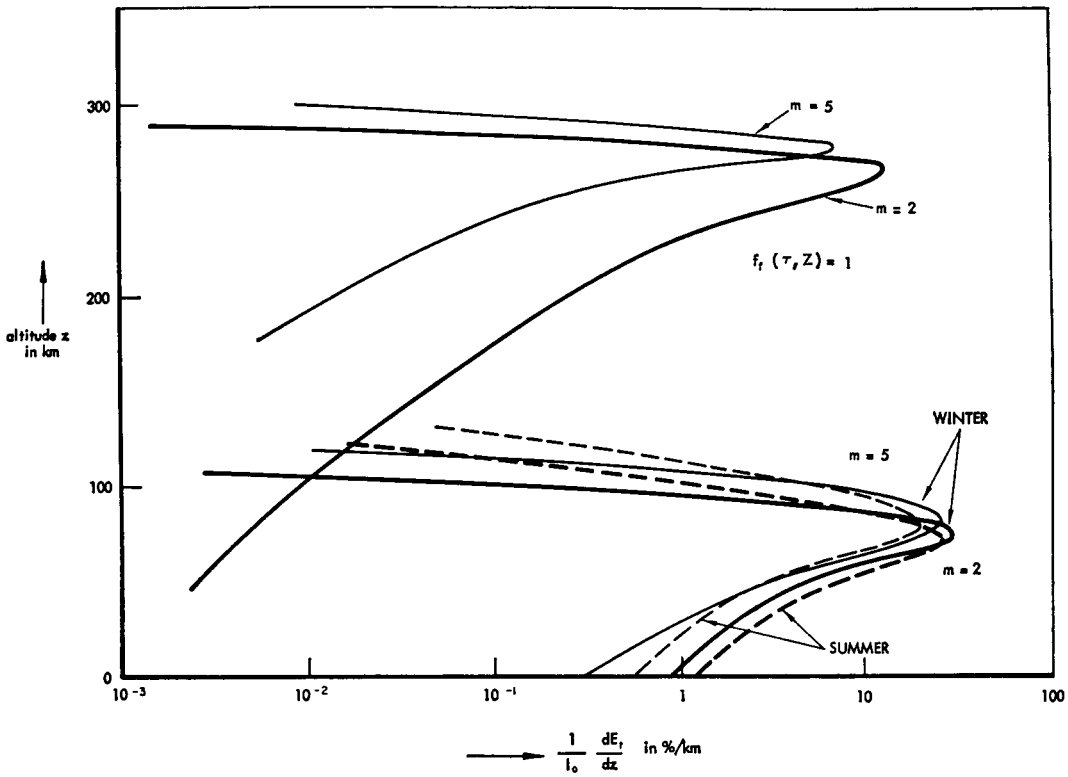

Fig. 12. Relative dissipation rate of energy flux transferred by atmospheric acoustic waves, $(dE_t/dz)/I_0$ in %/km, where $I_0 = I_0(u)$ is the acoustic output at source as shown in Figure 10. Solid lines and dashed lines correspond to wintertime and summertime polar atmosphere, respectively; heavy and light lines stand for flat spectrum ($m = 2$) and steep spectrum ($m = 5$) of the waves, respectively.

differential frequency spectrum of the wave $i(\omega)$ will be assumed to be

$$i(\omega) = i_0\omega^{-m} \qquad m > 1 \qquad (21)$$

From Figures 5 and 6, the lower limit of the integral in (20), ω_A, is to be taken as follows:

Summer:

$$\omega_A = \omega_A(z) \quad \text{for} \quad 0 \leq z < 20 \text{ km}$$
$$0.023 \quad \text{for} \quad 20 \leq z < 70 \text{ km}$$
$$\omega_A(z) \quad \text{for} \quad 70 \leq z < 85 \text{ km}$$
$$0.025 \quad \text{for} \quad z \geq 85 \text{ km}$$

Winter:

$$\omega_A = \omega_A(z) \quad \text{for} \quad 0 \leq z < 30 \text{ km}$$
$$0.024 \quad \text{for} \quad z \geq 30 \text{ km}$$

Strictly speaking, the right-hand side of (20) should be multiplied by a geometrical factor which is inversely proportional to the distance from the source. The width of the source, the polar night jet stream, is more than several hundred kilometers [*Krishnamurti*, 1959] and the boundary is widely diffused horizontally. For this reason, the geometric attenuation factor is not important and can be neglected in the present approximation.

A constant i_0 in (21) is given by

$$I_0 = \int_{\omega_A(z_0)}^{\infty} i_0\omega^{-m}\, d\omega = i_0 \frac{{\omega_A}^{m-1}}{m-1} \qquad m > 1$$

where $I_0 = I_0(u)$ is the output power of acoustic waves at the level of source z_0 given by (17) and shown in Figure 10.

In Figure 12, the upper two curves of the relative dissipation rate of energy $(dE_t/dz)/I_0$

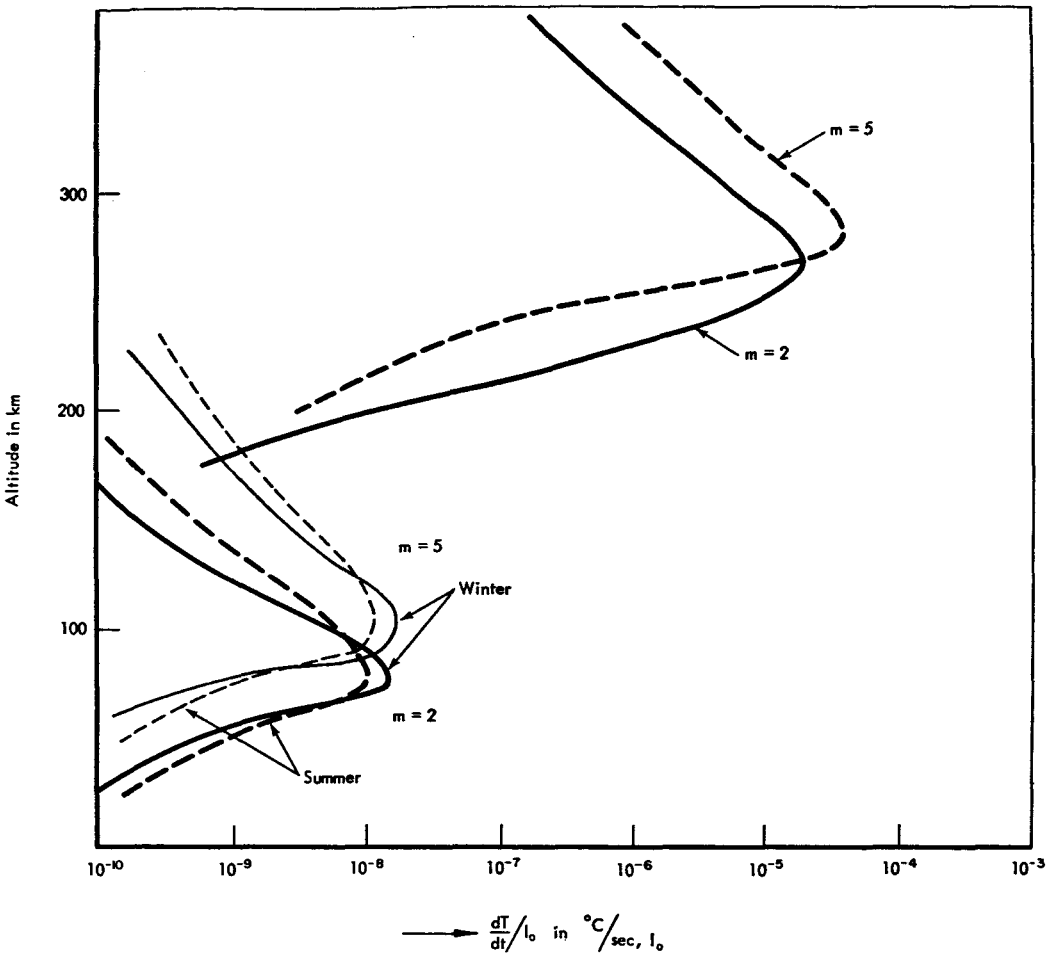

Fig. 13. The rate of atmospheric heating $dT(z)/dt$, °C/sec, in each layer due to the dissipation of acoustic energy flux I_0 (ergs/cm² sec) versus altitude z. Solid, dashed, heavy, and light lines correspond to those in Figure 12.

versus altitude are calculated by neglecting the transmissivity of the atmosphere; i.e., $f_t(\omega, z)$ is assumed unity. This corresponds to the estimation made by *Golitsyn* [1961*b*].

If all those dissipated energies of acoustic pressure waves are assumed to be converted into thermal energies of air, the rate of heating at each level is given by

$$\frac{dT(z)}{dt} \cong \frac{1}{C_p \rho(z)} \cdot \frac{1}{J_0} \frac{dE_t}{dz}$$

where $\rho(z)$ is mean atmospheric density at the altitude z.

The results shown in Figure 13 correspond to Figure 12 for a unit output power of the source, and, since the latter is shown in Figure 10, the following points can be made:

1. If the wind velocity around the 25-km level is of the order of 30 m/sec, as in the usual summertime polar stratosphere, then, from Figure 10, the acoustic power at the source is less than the order of 10^{-5} erg/cm² sec. Therefore, the rate of maximum heating, dT/dt is of the order of $10^{-8} \times 10^{-5}$ °C/sec or 10^{-3} °C/day at the maximum, of which the height is around 75 km if the wave spectrum is flat ($m = 2$), or 100 km if the spectrum is steep ($m = 5$), respectively.

2. On the other hand, if the wind velocity around 25 km exceeds 100 m/sec (which is

steadily observed in the polar night jet stream [*Krishnamurti*, 1959; *Riehl*, 1962]), the output power I_0 is between 10^3 and 1 erg/cm^2 sec, as can be seen from Figure 10. The corresponding maximum warming rate is then $2 \times (10^{-5} \sim 10^{-8})$ °C/sec or $2 \times (1 \sim 10^{-3})$ °C/day at the altitude of 75 km for $m = 2$, or around 100 km for $m = 5$, respectively.

3. If the transmissivity of the atmosphere is disregarded, as for Golitsyn's estimate, then, from the two upper curves shown in Figure 13, the rate of maximum heating is of the order of 10^{-10} °C/sec (10^{-5} °C/day) in summer, and 10^{-2} to 10^{-5} (10^3 — 1 °C/day) in winter. The height of maximum heating is around 260 to 300 km, corresponding to $m = 2$ to 5.

Conclusion

Although the available estimates of the acoustic energy flux for upper air heating have a wide range (Figure 10) due to ambiguities of several parameters, such as the mean velocity of turbulent motion around the jet stream, the effective size of eddy in this turbulence, and the frequency spectrum of turbulently produced acoustic waves, the following remarks can be made from present calculations:

1. Owing to the temperature gradient, the atmosphere above the 100-km level is not transparent for atmospheric acoustic waves, especially long waves. Therefore acoustic heating is most effective for warming the 100-km level rather than 200- and 300-km levels (Figure 13).

2. On the other hand, if the transmissivity of sound waves due to thermal gradient in the atmosphere is disregarded, most heating occurs around the 300-km level, and its rate exceeds 10°C/day in winter.

3. Although the acoustic power from polar night jet stream is more than 2 orders of magnitude larger than that of a tropospheric disturbance, acoustic heating around the mesopause is not sufficient to compensate for the cooling rate (about 10°C/day) of these levels in winter.

4. In this respect, another mechanism of dynamical heating such as energy transfer by means of internal gravity waves [*Hines*, 1963] might be effective for such warmings of the mesosphere as those observed by *Nordberg and Smith* [1963].

5. If the wind velocity of the jet stream continually exceeds more than 200 m/sec, the layer around the mesopause can be warmed significantly even by acoustic waves.

Note added in proof: The relative transmissivity of atmospheric acoustic waves, $f_t(\tau, z)$, is more accurately given by

$$f_t(\tau, z) \cong 1 - \cos \theta_c(\tau, z)$$

where

$$\theta_c(\tau, z) \cong \sin^{-1} \frac{k_c(\tau, z_0)}{k_c(\tau, z)}$$

and $k_c(\tau, z)$ is the maximum horizontal wave number at the height z for a given period τ, and z_0 is the height of minimum atmospheric temperature.

However, there is no essential difference in the general trend of $f_t(\tau, z)$ with altitude z as shown in Figure 9, even if more rigorous transmissivity is required.

References

Batchelor, G. K., and H. Bondi, *The Theory of Homogeneous Turbulence*, Cambridge University Press, London, 1956.

Blamont, J. E., and C. De Jager, Upper atmospheric turbulence near the 100-km level, *Ann. Geophys., 17*, 134–144, 1961.

Boville, B. W., C. V. Wilson, and F. K. Hare, Baroclinic waves of the polar night vortex, *J. Meteor., 18*, 567–580, 1961.

Charney, J. G., and Y. G. Drazin, Propagation of planetary scale disturbances from the lower into the upper atmosphere, *J. Geophys. Res., 66*, 83–110, 1961.

Cook, R. K., and J. M. Young, Microbaroms and sound radiated by ocean waves (abstract), *Trans. Am. Geophys. Union, 44*(1), 42, 1963.

Daniels, F. B., Acoustic energy generated by ocean waves, *J. Acoust. Soc. Am., 24*, 83, 1952.

Eckart, C., The theory of noise in continuous media, *J. Acoust. Soc. Am., 25*, 195–199, 1953.

Eckart, C., *Hydrodynamics of Oceans and Atmospheres*, Pergamon Press, London, 1960.

Golitsyn, G. S., On absorption of sound in the atmosphere and ionosphere, *Bull. Acad. Sci. USSR, English Transl.*, No. 6, 618–621, 1961*a*.

Golitsyn, G. S., The possibility of heating the upper atmosphere by long-wave acoustic radiation, *Bull. Acad. Sci. USSR, English Transl.*, No. 7, 720–721, 1961*b*.

Gossard, E. E., Vertical flux of energy into the lower ionosphere from internal gravity waves generated in the troposphere, *J. Geophys. Res., 67*, 745–757, 1962.

Haurwitz, B., Frictional effects and the meridional circulation in the mesosphere, *J. Geophys. Res., 66*, 2381–2391, 1961.

Heisenberg, W., On the theory of statistical and isotropic turbulence, *Proc. Roy. Soc. London, A, 195*, 402–406, 1948.

Hines, C. O., Internal atmospheric gravity waves at ionospheric heights, *Can. J. Phys., 38*, 1441–1481, 1960.

Hines, C. O., Comments at Annual Meeting, Am. Geophys. Union, April 1962.

Hines, C. O., The upper atmosphere in motion, *Quart. J. Roy. Meteorol. Soc., 89,* 1–42, 1963.

Hines, C. O., Dynamical heating of the atmosphere at ionospheric heights (abstract), *Trans. Am. Geophys. Union, 44*(1), 34, 1963.

Ishikawa, G., Solar corpuscular radiation as a heat source of the upper atmosphere, *Papers Meteorol. Geophys. Tokyo, 10,* 93–123, 1959.

Kellogg, W. W., Warming of the polar mesosphere and lower ionosphere in winter, *Rand Corp. Tech. Rept. P-2032-NSF,* July 5, 1960.

Kellogg, W. W., Chemical heating above the polar mesopause in winter, *J. Meteorol., 18,* 373–381, 1961.

Kochanski, A., Circulation and temperatures at 70 to 100 kilometer height, *J. Geophys. Res., 68,* 213–226, 1963.

Krishnamurti, T. N., A vertical cross section through the 'polar-night' jet stream, *J. Geophys. Res., 64,* 1835–1844, 1959.

Kulsrud, R. M., Effect of magnetic fields on generation of noise by isotropic turbulence, *Astrophys. J., 120,* 461–480, 1954.

Lighthill, M. J., On sound generated aerodynamically, 1, General theory, *Proc. Roy. Soc. London, A, 211,* 564–587, 1951.

Lighthill, M. J., On sound generated aerodynamically, 2, Turbulence as a source of sound, *Proc. Roy. Soc. London, A, 222,* 1–32, 1954.

Maeda, K., On the heating of the polar upper atmosphere, *NASA Tech. Note TR-141,* 1962.

Maeda, K., Auroral dissociation of molecular oxygen in the polar mesosphere, *J. Geophys. Res., 68,* 185–197, 1963.

Martyn, D. F., Cellular atmospheric waves in the ionosphere and troposphere, *Proc. Roy. Soc. London, A, 201,* 216–233, 1950.

Nordberg, W., and W. Smith, Preliminary measurements of temperatures and winds above 50 km over Wallops Island, Virginia, *NASA Tech. Note D-1694,* March 1963.

Proudman, I., The generation of noise by isotropic turbulence, *Proc. Roy. Soc. London, A, 214,* 119–132, 1952.

Rayleigh, J. W. S., *The Theory of Sound,* 1929, republished by Dover Publications, New York, 1945.

Riehl, H., Jet streams of the atmosphere, *Tech. Rept. 32, Dept. Atmospheric Sci.,* Colorado State University, May 1962.

Schatzman, E., Spherically symmetric motions in stellar atmospheres, B, The propagation of a short-wave in the atmosphere of varying density, *Nuovo Cimento, 22,* 209–226, 1961.

Schrödinger, E., Zur akustik der Atmosphäre, *Phys. Z., 18,* 445–453, 1917.

Stroud, W. G., W. Nordberg, and W. R. Bandeen, Rocket-grenade measurements of temperatures and winds in the mesosphere over Churchill, Canada, *J. Geophys. Res., 65,* 2307–2323, 1960.

Tolstoy, I., The theory of waves in stratified fluids including the effects of gravity and rotation, *Rev. Mod. Phys., 35,* 207–230, 1963.

U. S. Weather Bureau, *Daily 100 and 50 mb Three Times Monthly 30 mb Synoptic Weather Maps of the IGY Period,* U. S. Department of Commerce, Washington, 1961.

Young, C., and E. D. Epstein, Atomic oxygen in the polar winter mesosphere, *J. Atmospheric Sci., 19,* 435–443, 1962.

(Manuscript received January 2, 1964.)